

Redox-Driven Conductance Switching via Filament Formation and Dissolution in Carbon/Molecule/TiO₂/Ag Molecular Electronic Junctions[†]

Solomon Ssenyange, Haijun Yan, and Richard L. McCreery*

Department of Chemistry, The Ohio State University, 100 W 18th Avenue, Columbus, Ohio 43210

Received April 28, 2006. In Final Form: July 28, 2006

Carbon/molecule/TiO₂/Au molecular electronic junctions show robust conductance switching, in which a metastable high conductance state may be induced by a voltage pulse which results in redox reactions in the molecular and TiO₂ layers. When Ag is substituted for Au as the “top contact”, dramatically different current/voltage curves and switching behavior result. When the carbon substrate is biased negative, an apparent breakdown occurs, leading to a high conductance state which is stable for at least several hours. Upon scanning to positive bias, the conductance returns to a low state, and the cycle may be repeated hundreds of times. Similar effects are observed when Cu is substituted for Au and for three different molecular layers as well as “control” junctions of the type carbon/TiO₂/Ag/Au. The polarity of the “switching” is reversed when the Ag layer is between the carbon and molecular layers, and the conductance change is suppressed at low temperature. Pulse experiments show very erratic transitions between high and low conductivity states, particularly near the switching threshold. The results are consistent with a switching mechanism based on Ag or Cu oxidation, transport of their ions through the TiO₂, and reduction at the carbon to form a metal filament.

Introduction

A variety of molecular electronic junction structures have been investigated over approximately the past decade, with the general objective of investigating how electrons are transported through one or more molecules positioned between two conductors.^{1–4} Most studies to date involve metal/molecule/metal junctions, based on covalent or electrostatic bonds between the molecules and metals, such as Au/thiol^{5–7} and Langmuir–Blodgett structures.^{8–10} It is generally accepted that both the molecular structure and the “contact” between metal and molecule are important to the junction conductance.^{11–17} At least, the metal work function, the metal–molecule bond, the presence of dipoles, and the arrangement of metal atoms at the metal/molecule

interface are expected to significantly affect electron transport (ET) through a metal/molecule/metal junction, in addition to the molecular structure itself.

A phenomenon of particular scientific and practical importance in molecular junctions is “conductance switching”, in which the junction can be switched between two or more states with significantly different resistance. If the two states are at least metastable, the junction could be used as a memory device, conceivably as small as one molecule. The mechanism(s) of conductance switching have been the subject of numerous investigations, and are likely to involve a range of distinct phenomena. Several switching mechanisms that have been considered to date include redox reactions of organic molecules^{4,18–27}, conformation changes,^{28–31} transient breaking of molecule/substrate bonds,³² formation of metal filaments,³³ and reduction

[†] Part of the Electrochemistry special issue.

* To whom correspondence should be addressed. Tel.: 614-292-2021.

E-mail: mcCreery.2@osu.edu.

(1) Jortner, J.; Ratner, M. *Molecular Electronics*; Blackwell Science Ltd.: Cambridge, MA, 1997.

(2) Reed, M. A.; Tour, J. M. *Sci. Am.* **2000**, 86–93.

(3) Tour, J. M. *Acc. Chem. Res.* **2000**, 33, 791–804.

(4) McCreery, R. *Chem. Mater.* **2004**, 16, 4477–4496.

(5) Zhou, C.; Deshpande, M. R.; Reed, M. A.; Jones, L.; Tour, J. M. *Appl. Phys. Lett.* **1997**, 71, 611–613.

(6) *Molecular Nanoelectronics*; Reed, M. A., Lee, T., Eds.; American Scientific Publishers: Stevenson Ranch, CA, 2003.

(7) Cai, L. T.; Skulason, H.; Kushmerick, J. G.; Pollack, S. K.; Naciri, J.; Shashidhar, R.; Allara, D. L.; Mallouk, T. E.; Mayer, T. S. *J. Phys. Chem. B* **2004**, 108, 2827–2832.

(8) Collier, C. P.; Mattersteig, G.; Wong, E. W.; Luo, Y.; Beverly, K.; Sampaio, J.; Raymo, F. M.; Stoddart, J. F.; Heath, J. R. *Science* **2000**, 289, 1172–1175.

(9) Melosh, N. A.; Boukai, A.; Diana, F.; Gerardot, B.; Badolato, A.; Petroff, P. M.; Heath, J. R. *Science* **2003**, 300, 112–115.

(10) Metzger, R. M. *Chem. Rev.* **2003**, 103, 3803.

(11) Rakshit, T.; Liang, G.; Ghosh, A.; Datta, S. *Nano Lett.* **2004**, 4, 1803–1807.

(12) Xue, Y.; Ratner, M. A. *Phys. Rev. B* **2003**, 68, 115406–115418.

(13) Hutchison, G. R.; Ratner, M. A.; Marks, T. J.; Naaman, R. *J. Phys. Chem. B* **2001**, 105, 2881–2884.

(14) Burin, A. L.; Ratner, M. A. *J. Phys. Chem.* **2000**, 113, 3941–3944.

(15) Yaliraki, S. N.; Roitberg, A. E.; Gonzalez, C.; Mujica, V.; Ratner, M. A. *J. Phys. Chem.* **1999**, 111, 6997–7002.

(16) Ashkenasy, G.; Cahen, D.; Cohen, R.; Shanzer, A.; Vilan, A. *Acc. Chem. Res.* **2002**, 35, 121–128.

(17) Saloman, A.; Arad-Yellin, R.; Shanzer, A.; Karton, A.; Cahen, D. *J. Am. Chem. Soc.* **2004**, 126, 11648–11657.

(18) Wong, E. W.; Collier, C. P.; Behloradsky, M.; Raymo, F. M.; Stoddart, J. F.; Heath, J. R. *J. Am. Chem. Soc.* **2000**, 122, 5831–5840.

(19) Pease, A. R.; Jeppesen, J. O.; Stoddart, J. F.; Luo, Y.; Collier, C. P.; Heath, J. R. *Acc. Chem. Res.* **2001**, 34, 433–444.

(20) Luo, Y.; Collier, C. P.; Jeppesen, J. O.; Nielsen, K. A.; Delonno, E.; Ho, G.; Perkins, J.; Tseng, H.-R.; Yamamoto, T.; Stoddart, J. F.; Heath, J. R. *Chem. Phys. Chem.* **2002**, 3, 519–525.

(21) Nowak, A.; McCreery, R. *J. Am. Chem. Soc.* **2004**, 126, 16621–16631.

(22) McCreery, R.; Vishwanathan, U.; Kalakodimi, R. J.; Nowak, A. M. *Faraday Discuss.* **2006**, 131, 33–43.

(23) Solak, A. O.; Ranganathan, S.; Itoh, T.; McCreery, R. L. *Electrochem. Solid State Lett.* **2002**, 5, E43–E46.

(24) Bandhopadhyay, A.; Pal, A. J. *J. Phys. Chem. B* **2003**, 107, 2531–2536.

(25) Seminario, J. M.; De La Cruz, C. E.; Derosa, P. A. *J. Am. Chem. Soc.* **2001**, 123, 5616–5617.

(26) Reed, M. A.; Chen, J.; Rawlett, A. M.; Price, D. W.; Tour, J. M. *Appl. Phys. Lett.* **2001**, 78, 3735–3737.

(27) Dinglasan, J. A. M.; Michael Bailey, M.; Jong B. Park, J. B.; Dhirani, A.-A. *J. Am. Chem. Soc.* **2004**, 126, 6491–6497.

(28) Blum, A. S.; Kushmerick, J. G.; Long, D. P.; Patterson, C. H.; Yang, J. C.; Henderson, J. C.; Yao, Y.; Tour, J. M.; Shashidhar, R.; Ratna, R. R. *Nat. Mater.* **2005**, 4, 167–172.

(29) Donhauser, Z. J.; Mantooth, B. A.; Kelly, K. F.; Bumm, L. A.; Monnell, J. D.; Stapleton, J. J.; Price, D. W.; Rawlett, A. M.; Allara, D. L.; Tour, J. M.; Weiss, P. S. *Science* **2001**, 292, 2303–2307.

(30) Lewis, P.; Inman, C.; Yao, Y.; Tour, J.; Hutchinson, J.; Weiss, P. *J. Am. Chem. Soc.* **2004**, 126, 12214–12215.

(31) Lewis, P. A.; Inman, C. E.; Maya, F.; Tour, J. M.; Hutchison, J. E.; Weiss, P. S. *J. Am. Chem. Soc.* **2005**, 127, 17421–17426.

of metal ions to form metallic conductors.^{34,35} A mechanism involving redox reactions of metals inside the junction to form and break metallic “short circuits”^{36–40} is particularly relevant to the current work, as will be apparent later.

Although gold is used as the substrate and top contact in many junction paradigms,^{41–47} alternative structures include Au/molecule/Ti,^{5,8,18,48,49–52} Ag/molecule/Hg,^{53,54} Pt/molecule/Ti,^{49–52} Hg/molecule/Hg,^{55–57} as well as junctions with aluminum³³ or copper⁵⁸ as top contacts. A significant concern with such junctions is the possibility of forming metal filaments, or “short circuits”, by penetration of metal atoms through the molecular layer during fabrication or under an applied bias. Metal penetration through Au/thiol monolayers has been studied extensively,^{59–61} and dynamic formation of titanium filaments has been invoked to explain “switching” between high and low conductance states in Pt/molecule/Ti junctions.^{52,62} Our group has investigated carbon/molecule/metal junctions based on a covalent bond between a graphitic surface and aromatic molecules.^{4,21,58,63–66} The carbon is a pyrolyzed photoresist film

(PPF) resembling glassy carbon with a resistivity of $\sim 0.006 \Omega \cdot \text{cm}$ and a surface with an rms roughness of $< 5 \text{ \AA}$. Vapor deposition of a top contact of metal or metal oxide completes the molecular electronic junction. For example, PPF/biphenyl/Cu junctions show nonlinear current density/voltage (J/V) curves which depend strongly on molecular structure,⁵⁸ whereas PPF/nitroazobenzene/TiO₂/Au junctions are rectifiers which exhibit strong hysteresis.^{21,22,63,66,67} During the course of investigating PPF/molecule/TiO₂/Au and PPF/molecule/AlO_x/Au junctions, we observed redox behavior which greatly affected junction conductance. Structural changes in the molecular layer were verified by in situ Raman spectroscopy of junctions under bias, and two redox states which persisted for several minutes were identified.^{21,63} Nitroazobenzene (NAB) junctions containing either TiO₂ or AlO_x could be cycled between two spectroscopically distinct states several times, indicating the structural changes are at least partially reversible. We attribute the redox reactions occurring in solid state molecule/oxide layers only 5–8 nm thick to the high electric fields across the active region of the molecular junction.

The fact that junction conductance is strongly dependent on the presence of Al or Ti oxides is not surprising, given their low conductivity. However, the redox activity they promote may have substantial applications in molecular memory or related microelectronic devices. During the course of investigating junctions containing a metal oxide, we observed that the identity of the “top contact” metal (Au, Ag, Cu, Hg, and Ti) had strong effects on the electronic behavior for particular combinations of oxide and metal contact. The current paper describes a comparison of PPF/molecule/TiO₂/metal junctions with different “top contact” metals, including Au, Ag, Cu, and Ti, and concludes with a proposed mechanism for generating metal filaments by solid-state redox reactions.

Experimental Section

Molecular junctions were fabricated and tested as described in detail previously, using the “crossed junction” design.^{21,58,63} Briefly, 1 mm wide strips of PPF were prepared lithographically on a ~ 200 nm thick SiO₂ layer on silicon. Molecular layers of fluorene (FL, 1.7 nm thick) and nitroazobenzene (NAB, 4.5 nm thick) were deposited on the PPF by electrochemical reduction of the corresponding diazonium reagents. Strips of metal oxide and/or metal 0.5 mm wide were deposited through a shadow mask perpendicularly to the PPF strips by electron beam evaporation, to form a 0.5×1.0 mm junction (area = 0.005 cm²). TiO₂ was deposited from rutile in $\sim 1.5 \times 10^{-5}$ Torr of O₂, and Al₂O₃ was deposited from alumina granules. Deposition rates were as follows: TiO₂, 0.03 nm/s; Al₂O₃, 0.03 nm/s; Au, 0.1 nm/s; Ag, 0.1 nm/s; Cu, 0.1 nm/s. The metal and metal oxide thicknesses determined with a quartz crystal microbalance are given in parentheses in nanometers (e.g., PPF/FL(1.7)/TiO₂(5)/Au designates a 1.7 nm fluorene layer and a 5 nm thick TiO₂ layer). Ti metal was deposited at $\sim 1 \times 10^{-6}$ Torr, at a rate of 0.1 nm/s. All junctions had a final layer of 12 nm of Au to protect metals from oxidation.

Electronic testing occurred in air, with a “3-wire” configuration unless noted otherwise. The bias (PPF relative to Au) was applied between the PPF and Au strips through tungsten probes on 3-axis micromanipulators. Ohmic losses in the PPF were compensated in a “3-wire” configuration in which the iR-corrected bias was measured differentially between a tungsten probe on the undriven end of the

(32) Ramachandran, G. K.; Hopson, T. J.; Rawlett, A. M.; Nagahara, L. A.; Primak, A.; Lindsay, S. M. *Science* **2003**, *300*, 1413–1416.

(33) Richter, C. A.; Stewart, D. R.; Ohlberg, D. A. A.; Williams, R. S. *Appl. Phys.* **2005**, *80*, 1355–1362.

(34) Kozicki, M. N.; Park, M.; Mitkova, M. *IEEE Trans. Nanotechnol.* **2005**, *4*, 331–338.

(35) Mitkova, M.; Kozicki, M. N.; Kim, H. C.; Alford, T. L. *Thin Solid Films* **2004**, *449*, 248–253.

(36) Kozicki, M. N.; Mitkova, M.; Aberouette, J. P. *Physica E* **2003**, *19*, 161–166.

(37) Gilbert, N. E.; Gopalan, C.; Kozicki, M. N. *Solid-State Electron.* **2005**, *49*, 1813–1819.

(38) Kozicki, M. N.; Mitkova, M.; Park, M.; Balakrishnan, M.; Gopalan, C. *Superlattices Microstruct.* **2003**, *34*, 459–465.

(39) Mitkova, M.; Kozicki, M. N.; Kim, H. C.; Alford, T. L. *J. Non-Cryst. Solids* **2004**, *338–340*, 552–556.

(40) Terabe, K.; Hasegawa, T.; Nakayama, T.; Aono, M. *Lett. Nat.* **2005**, *433*, 47–50.

(41) Cui, X. D.; Primak, A.; Zarate, X.; Tomfohr, J.; Sankey, O. F.; Moore, A. L.; Moore, T. A.; Gust, D.; Harris, G.; Lindsay, S. M. *Science* **2001**, *294*, 571–574.

(42) Rawlett, A. M.; Hopson, T. J.; Nagahara, L. A.; Tsui, R. K.; Ramachandran, G. K.; Lindsay, S. M. *Appl. Phys. Lett.* **2002**, *81*, 3043–3045.

(43) Xu, B.; Tao, N. J. *Science* **2003**, *301*, 1221–1223.

(44) Xiao, X.; Xu, B.; Tao, N. J. *Nano Lett.* **2004**, *4*, 267–271.

(45) Chen, F.; He, J.; Nuckolls, C.; Roberts, T.; Klare, J.; Lindsay, S. M. *Nano Lett.* **2005**, *5*, 503–506.

(46) Wold, D. J.; Frisbie, C. D. *J. Am. Chem. Soc.* **2000**, *122*, 2970–2971.

(47) Wold, D. J.; Haag, R.; Rampi, M. A.; Frisbie, C. D. *J. Phys. Chem. B* **2002**, *106*, 2813.

(48) Chen, J.; Reed, M. A.; Rawlett, A. M.; Tour, J. M. *Science* **1999**, *286*, 1550–1552.

(49) Stewart, D. R.; Ohlberg, D. A. A.; Beck, P. A.; Lau, C. N.; Williams, R. S. *Appl. Phys. A: Mater. Sci. Process.* **2005**, *A80*, 1379–1383.

(50) Lau, C. N.; Stewart, D. R.; Bockrath, M.; Williams, R. S. *Appl. Phys. A: Mater. Sci. Process.* **2005**, *A80*, 1373–1378.

(51) Galperin, M.; Nitzan, A.; Ratner, M. A.; Stewart, D. R. *J. Phys. Chem. B* **2005**, *109*, 8519–8522.

(52) Lau, C. N.; Stewart, D. R.; Williams, R. S.; Bockrath, M. *Nano Lett.* **2004**, *4*, 569–572.

(53) Holmlin, R. E.; Haag, R.; Chabynyc, M. L.; Ismagilov, R. F.; Cohen, A. E.; Terfort, A.; Rampi, M. A.; Whitesides, G. M. *J. Am. Chem. Soc.* **2001**, *123*, 5075–5085.

(54) Haag, R.; Rampi, M. A.; Holmlin, R. E.; Whitesides, G. M. *J. Am. Chem. Soc.* **1999**, *121*, 7895–7906.

(55) Slowinski, K.; Majda, M. *J. Electroanal. Chem.* **2000**, *491*, 139–147.

(56) Slowinski, K.; Chamberlain, R. V.; Miller, C. J.; Majda, M. *J. Am. Chem. Soc.* **1997**, *119*, 11910–11919.

(57) Slowinski, K.; Fong, H. K. Y.; Majda, M. *J. Am. Chem. Soc.* **1999**, *121*, 7257–7261.

(58) Anariba, F.; Steach, J.; McCreery, R. J. *Phys. Chem. B* **2005**, *109*, 11163–11172.

(59) Haynie, B. C.; Walker, A. V.; Tighe, T. B.; Allara, D. L.; Winograd, N. *Appl. Surf. Sci.* **2003**, *203–204*, 433–436.

(60) Walker, A. V.; Tighe, T. B.; Cabarcos, O. M.; Reinard, M. D.; Haynie, B. C.; Uppili, S.; Winograd, N.; Allara, D. *J. Am. Chem. Soc.* **2004**, *126*, 3954–3963.

(61) Walker, A. V.; Tighe, T. B.; Haynie, B. C.; Uppili, S.; Winograd, N.; Allara, D. *J. Phys. Chem. B* **2005**, *109*, 11263–11272.

(62) Stewart, D. R.; Ohlberg, D. A. A.; Beck, P. A.; Chen, Y.; Williams, R. S.; Jeppesen, J. O.; Nielsen, K. A.; Stoddart, J. F. *Nano Lett.* **2004**, *4*, 133–136.

(63) Kalakodimi, R. P.; Nowak, A.; McCreery, R. L. *Chem. Mater.* **2005**, *17*, 4939–4948.

(64) McGovern, W. R.; Anariba, F.; McCreery, R. J. *Electrochem. Soc.* **2005**, *152*, E176–E183.

(65) Nowak, A. M.; McCreery, R. L. *Anal. Chem.* **2004**, *76*, 1089–1097.

(66) McCreery, R. L.; Dieringer, J.; Solak, A. O.; Snyder, B.; Nowak, A.; McGovern, W. R.; DuVall, S. *J. Am. Chem. Soc.* **2003**, *125*, 10748–10758.

PPF strip and system ground. Where noted, a 2-wire arrangement without the voltage monitor was used to avoid erratic behavior during current transients. Steps and spikes in the current caused sudden ohmic voltage losses in the PPF, which appeared as an erratic variation in the voltage axis when three wires were used.

A thick film of a Zn(II)porphyrin polymer was prepared thermally from a diethynyl Zn(II) dimethyl porphyrin as described elsewhere.⁶⁸ The porphyrin reagent, 5-(4-ethynylphenyl)-10,15-(4-ethynylphenyl)-20 dimethylporphyrinatozinc (II), was provided by Jon Lindsey at North Carolina State University. A 1–2 mM porphyrin reagent in THF was used for modification, with the uncertainty of concentration caused by the very small amounts of porphyrin reagent available. Prior to molecule introduction and subsequent heat treatment, the carbon film (PPF) was placed in a vial. The vial was sealed with a Teflon cap and purged with flowing Ar for 10 min through a syringe needle. A syringe containing the porphyrin solution was inserted through the Teflon cap, and several drops of the solution were placed onto the film. The solvent was then allowed to dry under a continued Ar purge. The vial was transferred to a hot plate at a temperature of approximately 425 °C and the film was heated for 3 min. The vial was removed from the hot plate and allowed to reach room temperature under Ar purge. THF was twice syringed into the vial and sonicated for 1 min to remove physisorbed porphyrin. The modified carbon film was finally dried with a stream of Ar and removed from the vial for the deposition of the various oxides and metals. The thickness of the polymer was approximately 20 nm but varied somewhat across a given sample.

Results and Discussion

Figure 1A shows a I/V curve for a PPF/NAB(4.5)/TiO₂(5)/Au(12) junction obtained at 100 V/s. The electronic behavior of such junctions has been discussed in detail,^{22,58,69} and Raman spectroscopy revealed that NAB is reduced to a quinoid form under negative bias (PPF relative to Au).^{21,63} The hysteresis and conductance changes have been attributed to a redox process between the NAB/NAB⁻ couple and Ti^{IV}/Ti^{III} oxide, resulting in modulation of conduction band electrons in the TiO₂. Figure 1B is a similar voltammogram from a PPF/NAB(4.5)/TiO₂(5)/Ag(9)/Au(12) junction with identical structure except for the addition of a 9 nm Ag layer between the TiO₂ and Au. As shown in Figure 1B, addition of Ag has little effect on the I/V curve for positive bias, with similar current density and hysteresis to that of the junction lacking Ag. For biases negative of approximately -1V, however, a sudden and erratic increase in current is observed, which results in irreversible changes in the junction electronic behavior (Figure 1C).

The apparent breakdown observed with the Ag containing junction always occurred for a bias negative of -2 V, although its onset varied between -1 and -2 V. Hundreds of junctions containing only Au for the top contact never showed breakdown for -3 V excursions, and many were tested to -4 or -5 V. Figure 2A compares PPF/NAB(4.5)/TiO₂(5)/Au junctions with and without Ag between the TiO₂ and Au. After the “breakdown” occurred in the Ag-containing junction at -1.5 V, the junction could be cycled between low resistance and high resistance states, with hysteresis indicated by the arrows in the Figure 2A. Cycling could be repeated many times, with the transition from low to high resistance occurring at ~+1.2 V, and the transition back to low resistance at ~-1.5 V. As shown in Figure 2B, the “switching” cycle is independent of scan rate for the 10–1000 V/s range. The switching was repeatable for more than 100–

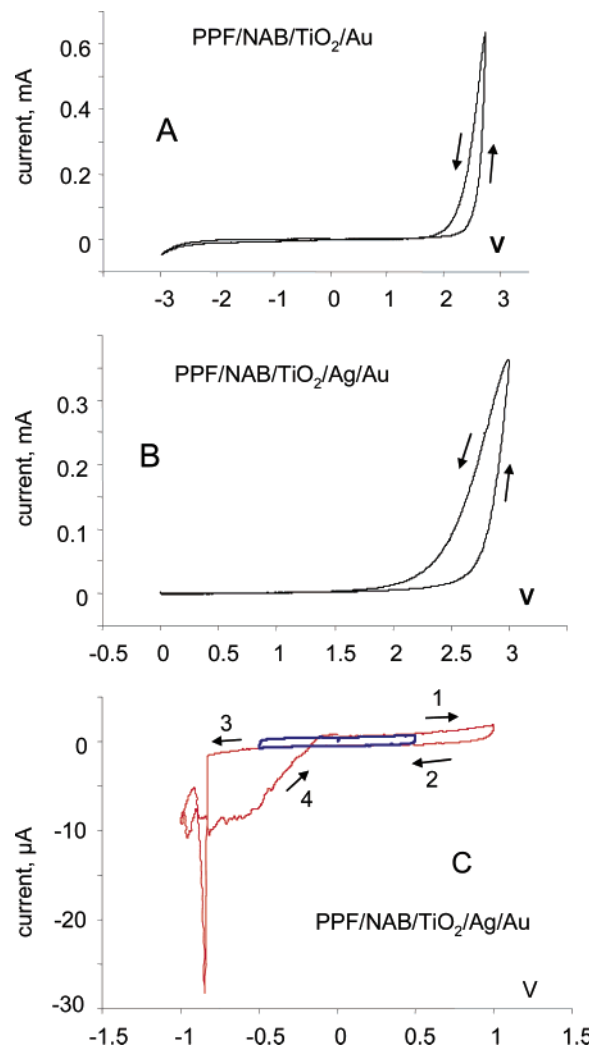


Figure 1. Current (I) vs voltage (V) curves for PPF/NAB(4.5)/TiO₂(5)/Au(12) junctions, obtained at 100 V/s, with scan direction indicated by arrows. B and C are results for junctions with an additional 9 nm layer of Ag between the TiO₂ and Au. The dark curve in C is a ± 0.5 V scan which preceded the red ± 1 V scan. The red scan was initiated in a positive direction, as indicated by the numbered arrows.

1000 complete cycles, although the cycle lifetime varied from junction to junction. The ratio of the resistance measured for $V = \pm 0.2$ V for the two states ranged from 10 to 100, although it often decreased slowly with repeated switching.

To explore the generality of the switching effect observed with NAB/TiO₂/Ag junctions, several variations in junction structure were examined. Comparison of PPF/TiO₂/Au and PPF/TiO₂/Ag/Au junctions (Figure 3A) shows that the molecular layer is not required for switching, but the Ag is. PPF/TiO₂(5)/Au junctions could be cycled hundreds of times between ± 2 V, with no change from the I/V curve of Figure 3A. However, PPF/TiO₂(5)/Ag(9)/Au(12) junctions consistently broke down for $V < -1.0$ V and then exhibited the hysteresis and cycling apparent in Figure 3A. Figure 3B shows that substitution of Ag with Ti, to make a PPF/NAB(4.5)/TiO₂(5)/Ti(5)/Au junction prevents the “breakdown” effect, although the conductance is higher than PPF/NAB(4.5)/TiO₂(5)/Au junctions made without metallic Ti. Figure 3C shows I/V curves from PPF/NAB(4.5)/TiO₂(5)/Cu(9)/Au junctions, with Cu substituted for Ag. Positive bias scans to +3 V (1 and 2) were repeatable without breakdown, whereas negative bias caused an abrupt current increase at ~ -2 V. As was the case with Ag, the Cu junctions could be cycled between

(67) McCreery, R.; Dieringer, J.; Solak, A. O.; Snyder, B.; Nowak, A. M.; McGovern, W. R.; DuVall, S. *J. Am. Chem. Soc.* **2004**, *126*, 6200.

(68) Liu, Z.-M.; Schmidt, I.; Thamyongkit, P.; Loewe, R. S.; Syomin, D.; R., D. J.; Zhao, Q.; Misra, V.; Lindsey, J. S.; Bocian, D. F. *Chem. Mater.* **2005**, *17*, 3728–3742.

(69) McCreery, R.; Wu, J.; Kalakodimi, R. J. *Phys. Chem. Chem. Phys.* **2006**, *8*, 2572–2590.

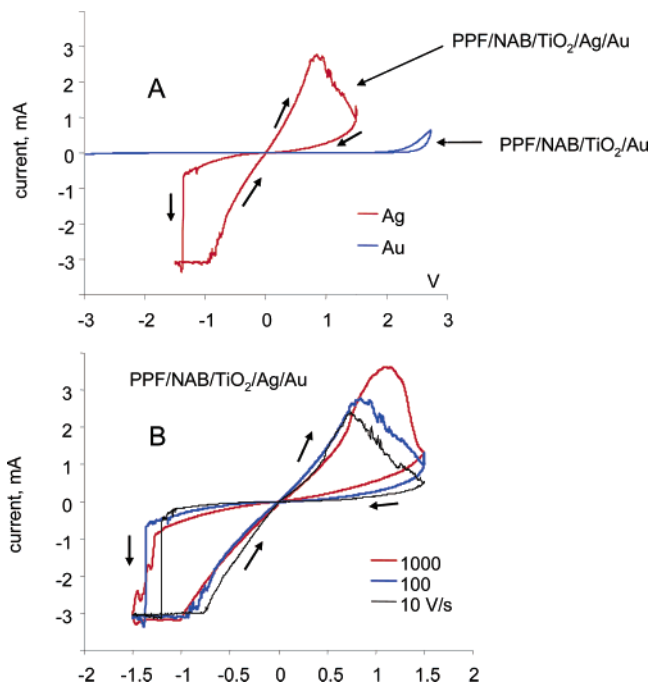


Figure 2. (A) I/V curves for PPF/NAB(4.5)/TiO₂(5)/Au(12) junctions at 100 V/s, with and without Ag present. Blue curve is the same as Figure 1A, red curve is a Ag junction after breakdown similar to that shown in Figure 1C. Arrows indicate scan direction. (B) PPF/NAB(4.5)/TiO₂(5)/Ag(9)/Au(12) junction after breakdown, at the indicated scan rates from 10 to 1000 V/s.

high and low resistance states for 10–100+ cycles, and the current was often erratic during cycling. The hysteresis exhibited the same pattern as that with Ag junctions, as indicated by the numbered arrows in Figure 3C. Figure 3D compares a PPF/FL(1.7)/TiO₂(5)/Ag(9)/Au(12) junction to its equivalent lacking Ag. The behavior is qualitatively similar to that observed with

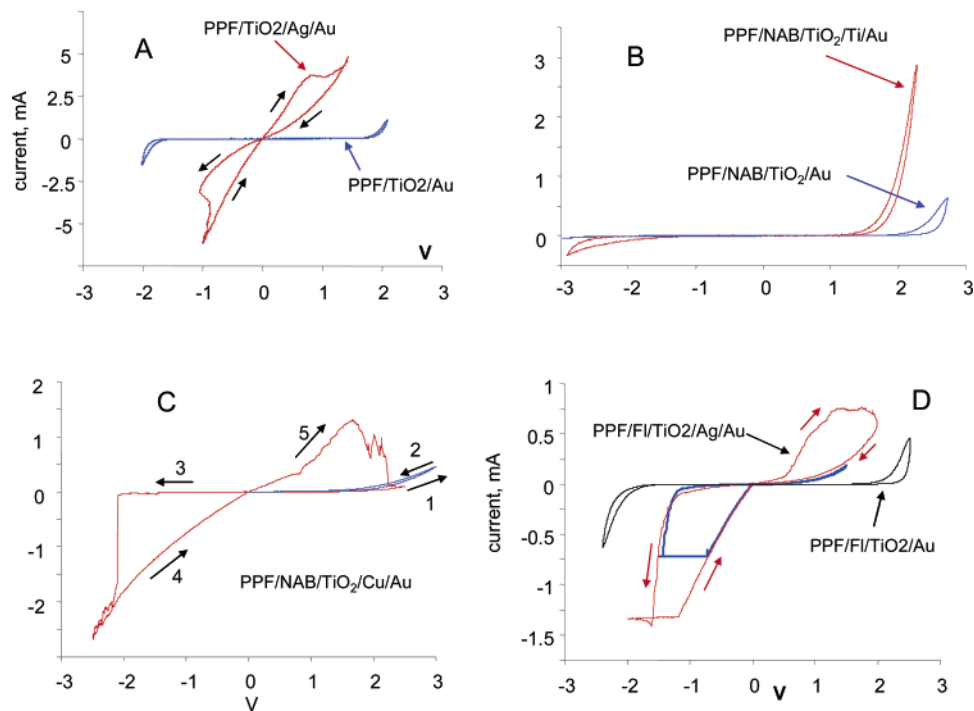


Figure 3. (A) Comparison of I/V curves for PPF/TiO₂(5)/Au(12) junctions with and without a 9 nm layer of Ag between TiO₂ and Au. (B) I/V curves for PPF/NAB(4.5)/TiO₂(5)/Au junctions with and without a 3 nm layer of Ti between TiO₂ and Au. (C) I/V curves for a PPF/NAB(4.5)/TiO₂(5)/Au(9)/Au(12) junction. Blue curves is initial scan between 0 and +3 V, red scan is ±3 V. Scans occurred in order and direction indicated. (D) PPF/FL(1.7)/TiO₂(5)/Au junctions with and without Ag between TiO₂ and Au. Blue scan is the first for the Ag junction, and was initiated in the positive direction. All I/V curves obtained at 100 V/s.

NAB, although fluorene does not exhibit rectification. The polarity of breakdown was consistent for PPF/molecule/TiO₂/Ag/Au junctions, occurring predominantly for negative bias in the range of −1 to −2 V. NAB/TiO₂/Ag junctions occasionally broke down at positive bias but always at significantly higher voltage magnitude than that causing breakdown during the negative scan.

To determine the origin of the breakdown polarity, an “inverted” junction was prepared with Ag between the PPF and NAB, i.e., PPF/Ag(5)/NAB/TiO₂(5)/Au(12). The NAB thickness was uncertain, but deposition conditions were similar to those which yielded 5 nm NAB films on PPF. As shown in Figure 4A, the “inverted” junction could be scanned to a bias of −3 V without breakdown. This bias is significantly negative of that causing breakdown in any of the PPF/molecule/TiO₂/Ag/Au junctions studied. Furthermore, a scan to *positive* bias caused breakdown, at ~+2 V in the case shown in Figure 4A. Once breakdown occurred, the inverted junction could be cycled between low and high resistance states (Figure 4B), but with hysteresis opposite to that shown in Figure 2B. The inverted junction switches from high resistance to low at ~+2 V, and from low resistance to high at approximately −2 V. To reiterate, the inverted PPF/Ag/NAB/TiO₂/Au junction shows opposite polarity from the PPF/NAB/TiO₂/Ag/Au junction with respect to breakdown, and the hysteresis loop is exactly opposite.

The reversal of polarity with the Ag on opposite sides of the NAB/TiO₂ layers indicates that breakdown is strongly favored when the Ag is biased positively relative to the PPF. As a working hypothesis, suppose a positive Ag bias oxidizes the Ag to Ag⁺, then drives the Ag⁺ ion through the molecule/TiO₂ layer. Once the Ag⁺ reaches the PPF, it should be reduced back to Ag metal, since the PPF is biased negative. In effect, the Ag⁺ is acting as an ionic charge carrier which matches part or all of the electronic current in the external circuit. A counter reaction at the PPF electrode, such as would occur in a conventional redox cell, may not be necessary if the field is high enough to create an image

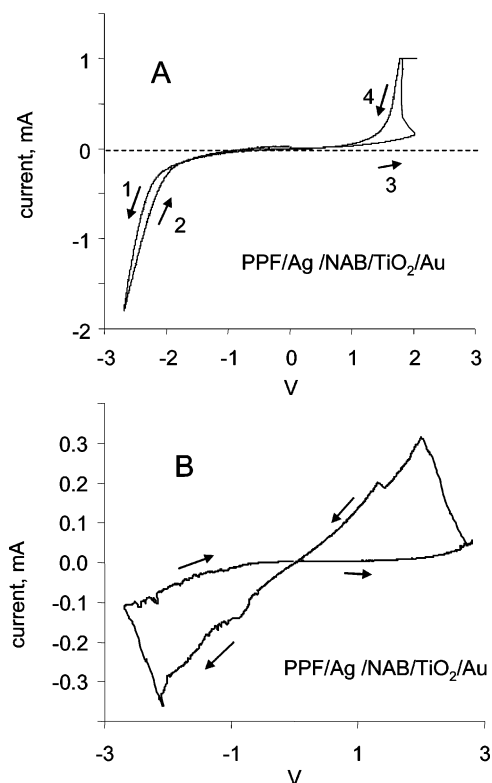


Figure 4. I/V curves for an “inverted” PPF/Ag(5)/NAB/TiO₂(5)/Au junction. (A) Scan initiated in negative direction (100 V/s) in order shown. (B) After breakdown.

charge in the PPF. The end result is transport of Ag metal from the positively biased Au/Ag electrode to the PPF. Once enough Ag has been transferred, Ag⁰ is likely to build up on the PPF, likely forming a Ag filament due to the higher local electric field near the tip of the growing filament. Filament growth would proceed until the TiO₂/molecule gap is bridged and a direct DC current path is provided, resulting in a significant increase in junction conductance. The fact that the PPF/TiO₂/Ag/Au junction also shows the switching effect indicates that the molecular layer may be largely irrelevant to the process, assuming Ag⁺ can penetrate both molecular and TiO₂ layers.

Figure 5 shows the switching effect on a third molecule, a Zn porphyrin polymer, with a thickness (~20 nm) greater than either FL (1.7) or NAB (4.5). Consistent with the previous results, the PPF/porphyrin/TiO₂/Ag/Au junction breaks down at about -1.5 V and can be cycled repeatedly between high and low resistance states. PPF/porphyrin/TiO₂(10)/Ag(9)/Au(12) junctions of the type shown in Figure 5 were cycled for 7500 complete cycles at 10 V/s with minor changes in the current density and hysteresis.

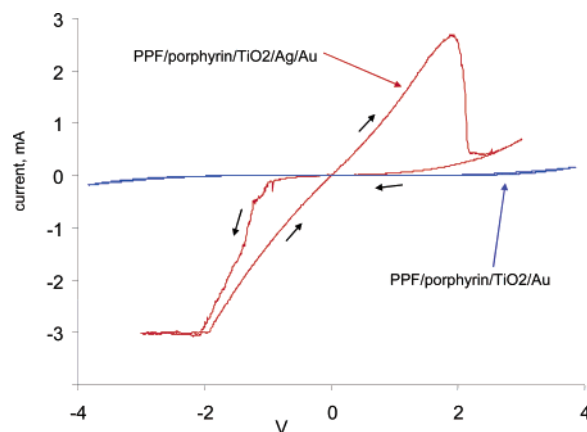


Figure 5. I/V curves for PPF/porphyrin(20)/TiO₂(10)/Au(12) junction with and without a 9 nm layer of Ag between the TiO₂ and Au; 100 V/s.

A junction similar to that yielding Figure 5, but with Al₂O₃ substituted for TiO₂, was investigated to determine if TiO₂ was required for “switching”. A PPF/porphyrin/Al₂O₃(5)/Au junction had very low current density, below 0.002 A/cm² for the range $V = \pm 4$ V. However, PPF/porphyrin/Al₂O₃(5)/Ag(9)/Au(12) junctions broke down in the range of -2 to -3 V and thereafter exhibited hysteresis similar to that of PPF/porphyrin/TiO₂/Ag/Au junctions.

Table 1 lists the observed resistance changes for several cases examined, demonstrating a decrease of at least a factor of 1000 upon “breakdown”. Table 1 also lists the cross-sectional area of Ag required to produce the observed resistance, assuming the filaments behave as expected for a bulk Ag conductor, with a resistivity equal to that of Ag, 1.6 μΩ·cm. For example, the PPF/NAB/TiO₂/Ag/Au junction resistance decreases from > 1 MΩ to 90.1 Ω after a negative voltage excursion caused filament formation. To produce a 90 Ω resistance through the 95 Å layer of TiO₂ and NAB would require a filament with an area of ~170 Å². This represents a fractional coverage of Ag of only ~3 × 10⁻¹² if the filaments act like bulk Ag. If we instead assume that each filament has the quantum mechanically limited conductance^{40,70} of (12.9 kΩ)⁻¹, only ~150 filaments are required to yield the observed resistance. In either case, the total cross sectional area of filaments is a tiny fraction of the junction area, and such filaments would be difficult to characterize by any spectroscopic technique. The only example of physical evidence for filament formation of which we are aware is scanning probe microscopy of filaments in Pt/molecule/Ti junctions reported by Lau et al.⁵⁰ XPS depth profiling of the current PPF/TiO₂/Ag/Au junctions was carried out after extensive voltage cycling, and the Ag penetrated deeper into the junction (see the Supporting

Table 1. Silver Filament Area Required to Yield Observed Junction Resistance

junction	figure	observed resistance	thickness, ^a Å	Ag area, ^b cm ²	Ag area, ^b Å ²	fractional coverage of filaments
Initial						
PPF/NAB/TiO ₂ /Ag/Au	1A	> 1 MΩ ^c	95	7.8 × 10 ⁻¹⁹	0.01	2 × 10 ⁻¹⁶
PPF/TiO ₂ /Ag/Au	3A	> 200 kΩ ^c	50	3.6 × 10 ⁻¹⁸	0.04	7 × 10 ⁻¹⁶
PPF/FL/TiO ₂ /Ag/Au	3D	> 500 kΩ ^c	70	2.0 × 10 ⁻¹⁸	0.02	4 × 10 ⁻¹⁶
After “Breakdown”						
PPF/NAB/TiO ₂ /Ag/Au	2B	90.1	95	1.7 × 10 ⁻¹⁴	168.7	3 × 10 ⁻¹²
PPF/TiO ₂ /Ag/Au	3A	272	50	3.0 × 10 ⁻¹⁵	29.4	5 × 10 ⁻¹³
PPF/FL/TiO ₂ /Ag/Au	3D	440	70	2.5 × 10 ⁻¹⁵	25.5	5 × 10 ⁻¹³

^a Thickness of molecular layer, if present, and TiO₂. ^b Cross sectional area of Ag calculated from observed resistance and the resistivity of Ag, 1.6 μΩ·cm, assuming filaments behave like bulk Ag. ^c Actual resistance significantly higher⁶⁹ but was not determined due to dynamic range limitations on the current amplifier.

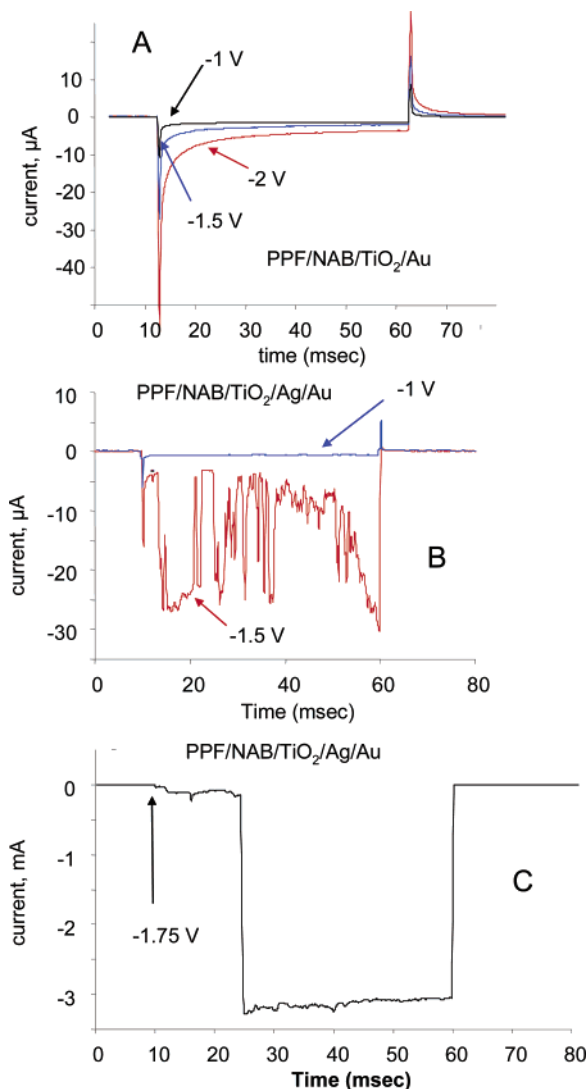


Figure 6. Current vs time results for PPF/NAB/TiO₂/Au junctions with and without Ag for voltage pulses from $V = 0$ to the indicated voltage at $t = 10$ ms then returned to $V = 0$ at $t = 60$ ms. (A) PPF/NAB(4.5)/TiO₂(5)/Au junction for three pulse voltages (B) PPF/NAB(4.5)/TiO₂(5)/Ag(9)/Au(12) junction for $V = -1$ and -1.5 V. (C) Same as B but for -1.75 V pulse; note large change in current scale.

Information), but such results are not conclusive due to disturbance of the Ag depth profile by argon ion sputtering.

The intermittent onset of switching is more obvious in the pulse experiments shown in Figure 6. Negative voltage pulses were applied to resting junctions and the transient current was recorded. For -1.0 to -2.0 V pulses on a PPF/NAB(4.5)/TiO₂(5)/Au junction, a smooth current decay was observed, at least part of which is capacitive charging current. As noted previously, the RC time constant for a junction acting as a parallel plate capacitor is a few microseconds, much shorter than the observed decay.^{63,66} This response could be repeated for hundreds of pulses, with only minor variability in pulse shape and magnitude. For a -1.5 V pulse to a PPF/NAB(4.5)/TiO₂/Ag junction, however, an erratic current response occurs, which varies in fine structure from pulse to pulse (Figure 6B). As the pulse voltage amplitude becomes more negative, the current increases rapidly to ~ 0.6 A/cm² at -1.75 V, and becomes less erratic (Figure 6C). The nature and implications of the pulse response are beyond the

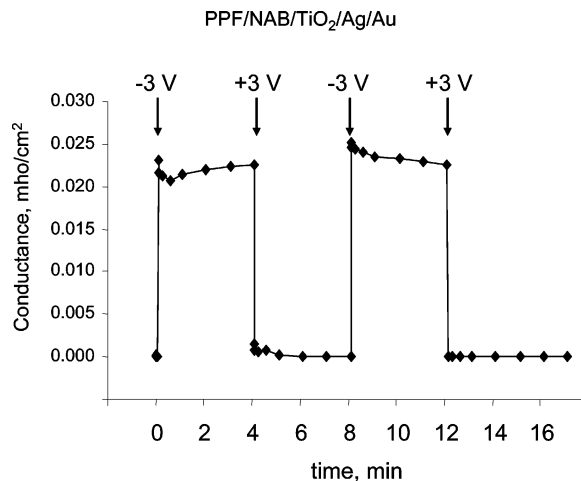


Figure 7. Conductance of a PPF/NAB(4.5)/TiO₂(5)/Ag(9)/Au(12) junction, measured as the slope of I/V curve for $V = \pm 0.2$ V. Starting with a new junction at $t = 0$, 100 ms voltage pulses were applied at the times indicated. Each point results from a ± 0.2 V scan at various times between pulses.

scope of the current work, and the important observation is the fundamentally distinct response when Ag is present in the junction.

Once the molecule/Ag junction is switched into its high or low resistance state, the junction conductance is quite stable with time. Figure 7 shows results from a PPF/NAB(4.5)/TiO₂(5)/Ag(9)/Au(12) junction plotted as conductance vs time. The conductance was measured as the slope of the I/V curve for $V = \pm 0.2$ V. At the times indicated, 100 ms pulses of the indicated voltage were applied, which switched the junction between its high and low conductance states. Both states were stable during repeated voltage scans, provided the voltage was restricted to the ± 1 V range. The PPF/FL/TiO₂/Ag/Au junction shown had a mean high/low conductance ratio of 65, although this ratio varied from junction to junction in the range of 10–100. Both the high and low conductance states were stable with time, lasting at least 6 h with a conductance change of $< 10\%$.

The “switching” behavior observed with Ag or Cu in the PPF/molecule/TiO₂/metal junctions is qualitatively and mechanistically distinct from that of solid-state junction designs we have reported previously.^{21,63,69} PPF/molecule/TiO₂/Au and PPF/molecule/AlO_x/Au junctions did not exhibit the sudden transients and erratic behavior apparent in Figures 1C and 4–6, and ± 3 V scans were repeatable and stable. The PPF/molecule/Cu junctions lacking TiO₂ had much lower resistance than the current junctions, and higher current densities (e.g., ~ 5 A/cm² at 0.5 V for PPF/FL/Cu/Au).⁵⁸ Presumably, the more conductive junctions lacking TiO₂ cannot support the high electric fields required to produce redox reactions in the junction. It is possible that the PPF/molecule/Hg junctions which exhibit qualitatively similar behavior to that shown in Figure 2B may involve redox events, but the Hg did not show the erratic current behavior of Figures 1 and 6.^{23,71}

The observations that “switching” occurs initially when the Ag or Cu is positively biased, leads to a persistent increase in junction conductance, and occurs more readily for the less noble Cu and Ag than for Au are all consistent with a redox-driven migration of Ag or Cu from positively biased electrode, as shown schematically in Figure 8. As proposed earlier, the metal cation produced at the positively biased electrode is driven through the junction by the high electric field and then reduced back to the

(70) Zahid, F.; Paulsson, M.; Datta, S. *Electrical Conduction through Molecules*; Academic Press: New York, 2003.

(71) Ranganathan, S.; Steidel, I.; Anariba, F.; McCreery, R. L. *Nano Lett.* **2001**, *1*, 491–494.

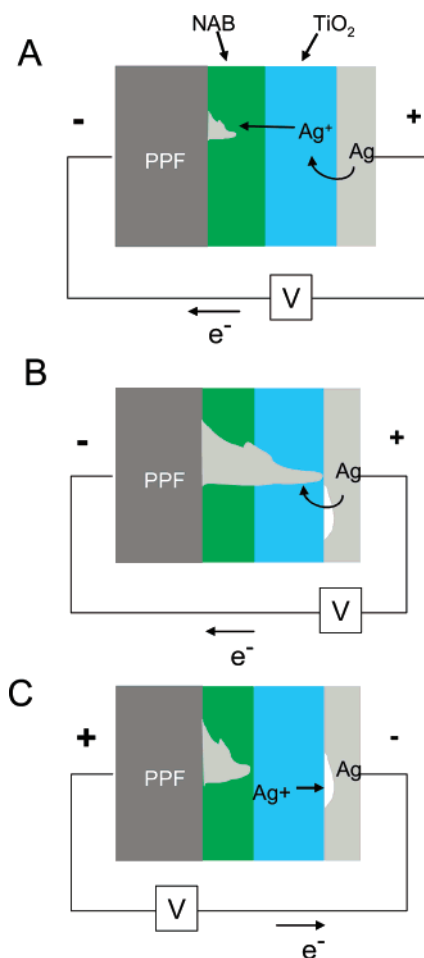


Figure 8. Schematic of proposed mechanism for Ag filament formation in PPF/molecule/TiO₂/Ag/Au junctions. A and B are for negative bias, and C is for positive (PPF relative to Au).

metal at the PPF surface. As a metal filament begins to form, the local electric field is increased at its tip, and additional metal ions should be reduced preferentially at the growing filament. When the filament reaches the positive electrode, a large increase in current occurs due to electronic conduction, and the field is dissipated, at least locally. Once the filament is formed, it is apparently stable for low bias ($|V| < 1\text{ V}$), for a few minutes to several hours, to produce the behavior shown in Figure 7. When the bias is reversed and the PPF becomes sufficiently positive ($> 1.5\text{ V}$), the filament is presumably oxidized and the metal returns to its initial location. Lowering the junction temperature significantly increased the bias required to cause breakdown (see the Supporting Information), consistent with a thermally activated redox reaction. This process of formation and removal of the Ag or Cu filaments was repeatable at least hundreds of cycles, although disordering and roughening of the metal surface is certain to occur.

Ag⁺ and Cu²⁺ are relatively small ions, and are known to permeate crystals interstitially. The well-known Ag₂S sulfide ion selective electrode is an example of Ag⁺ transport through a polycrystalline solid. A memory device with some characteristics in common with PPF/NAB/TiO₂/Ag junctions has been reported,^{34–39} in which Ag⁺ or Cu²⁺ are transported through a chalcogenide, Ge–S or tungsten oxide glass, and reduced in the junction to form a conductive path. Both the molecular layer and TiO₂ in the present junctions are disordered and very thin, so transport of small cations in a high electric field ($\sim 2\text{ MV/cm}$ at 2 V) is likely. We showed previously with Raman spectroscopy that redox reactions occur in PPF/NAB/TiO₂/Au and PPF/NAB/

AlO_x/Au junctions.^{21,63} Although there is not yet direct evidence of Ag or Cu oxidation in the current junctions, both oxidation and transport are feasible, and have been demonstrated in structurally similar devices.

Au by itself does not exhibit “switching” or current transients, indicating either that its redox potential is too high, or that its ions do not permeate TiO₂ or Al₂O₃. We proposed that the image charge in the Au surface may be adequate to support redox reactions at the PPF surface, although it is difficult to rule out motion of adventitious ions in this case. When Ti is present as Ti⁰, Ti^{II}, or Ti^{III} between the TiO₂ and Au (Figure 3B), there is no evidence for filament formation, even for $V = -3\text{ V}$. The larger currents with reduced Ti compared to the TiO₂-only case implies that reduced Ti provides mobile electrons, but “breakdown” is not observed even for $V \leq -3\text{ V}$. Ti is very unlikely to exist as atomic Ti⁰ or bare Ti²⁺, and its strong bonds to oxygen may prevent transport through the TiO₂ film.

The consequences of the current findings to both electrochemistry and molecular electronics are substantial, although somewhat indirect. They provide several more examples of redox reactions occurring in a 5–10 nm gap between two conductors, in this case the oxidation and reduction of metals.⁷² Solid-state electrochemistry is well-known in several contexts,⁷² although not in such thin films to the authors’ knowledge. The electric fields and potentials present in the current junctions approximate those found in electrochemical double layers at electrodes in electrolyte solution, so sufficient driving force for redox reactions should be available. The presence of adventitious ions from residual water or other reagents is difficult to rule out, but conversely, counterion motion may not be necessary beyond the metal ion itself moving from the negative to positive electrodes. As mentioned earlier, transport of Ag⁺ or Cu²⁺ through nanocrystalline TiO₂ and a disordered molecular film is certainly possible, given their transport through denser and more ordered materials such as sulfides and oxide glasses. Given the possibility of trace water, oxygen or carbon dioxide in the junctions, it is difficult to rule out ion formation and transport accompanying filament formation. As noted previously,^{21,63,66,69} the solid-state junction may have properties of both a parallel plate capacitor and a complete redox cell, with trace ions responding to the applied bias.

With the exception of intentional filament formation in solid state memory devices, filaments are generally undesirable in molecular electronic components. In most cases, filaments are destructive, and mask the effects of molecular structure and dynamics on the electronic behavior of molecular junctions. The current results indicate that Cu and Ag are prone to forming filaments when a high electric field is present, although there is no evidence that Cu forms filaments in the absence of an oxide. For example, PPF/fluorene/Cu/Au junctions could be cycled $> 10^8$ cycles between $\pm 0.6\text{ V}$ without observable changes, achieving current densities of $\sim 5\text{ A/cm}^2$ on each cycle.^{58,73} Nevertheless, caution is advisable when using Ag and Cu in molecular junctions. Au and Ti did not form observable filaments under the conditions examined herein, although Ti oxidation is quite likely given its negative redox potential. The absence of erratic current transients in junctions containing Au and Ti is evidence that filaments are not forming dynamically, and also were probably not present following junction fabrication. Given the tendency of Ti to form

(72) Riess, I. Comparison between Liquid State and Solid-State Electron chemistry. In *Encyclopedia of Electrochemistry*; Bard, A., Stratman, M., Eds.; Dekker: New York, 2003; Vol. 1, pp 253–281.

(73) Steach, J. Fabrication and Electrical Characterization of Carbon-based Crossbar Molecular Electronic Junctions, Ohio State University, 2005.

oxides with three oxidation states, the conditions of Ti deposition undoubtedly will affect the stability of Ti layers in molecular junctions.

Acknowledgment. This work was supported by the National Science Foundation through Project 0211693 from the Analytical and Surface Chemistry Division and by ZettaCore, Inc. The authors thank Jon Lindsey for providing the porphyrin reagent,

ZettaCore for technical assistance, and Jing Wu for correlative data on TiO₂/Au junctions.

Supporting Information Available: Temperature dependence of “breakdown” (Figures S1–S4). This material is available free of charge via the Internet at <http://pubs.acs.org>.

LA061153O